Published in final edited form as:
Neuron. 2012 April 26; 74(2): 410–422. doi:10.1016/j.neuron.2012.02.031.

Effects of cue-triggered expectation on cortical processing of taste

Chad L. Samuelsen[1,*], **Matthew P.H. Gardner**[1,2,*], and **Alfredo Fontanini**[1,2]

[1]Department of Neurobiology and Behavior, State University of New York at Stony Brook, Stony Brook, NY 11794

[2]Graduate Program in Neuroscience, State University of New York at Stony Brook, Stony Brook, NY 11794

SUMMARY

Animals are not passive spectators of the sensory world in which they live. In natural conditions they often sense objects on the bases of expectations initiated by predictive cues. Expectation profoundly modulates neural activity by altering the background state of cortical networks and modulating sensory processing. The link between these two effects is not known. Here, we studied how cue-triggered expectation of stimulus availability influences processing of sensory stimuli in the gustatory cortex (GC). We found that expected tastants were coded more rapidly than unexpected stimuli. The faster onset of sensory coding related to anticipatory priming of GC by associative auditory cues. Simultaneous recordings and pharmacological manipulations of GC and basolateral amygdala revealed the role of top-down inputs in mediating the effects of anticipatory cues. Altogether these data provide a new model for how cue-triggered expectation changes the state of sensory cortices to achieve rapid processing of natural stimuli.

Keywords

insular cortex; gustatory cortex; basolateral amygdala; top-down; behavior; emotion; sensory coding

INTRODUCTION

Food does not appear in the mouth unexpectedly. Tasting a food is typically the outcome of a behavioral sequence promoted by anticipatory cues. The sight of a dish, its odor or the sound of a beverage being poured are all signals that trigger expectations about the availability of a gustatory stimulus. As a result gustatory information is often perceived against the background of prior expectations.

Given the intimate relationship between taste and expectation, it comes as no surprise that this subject has been the focus of increasing attention. Manipulating anticipation and uncertainty significantly alters detection thresholds, intensity and hedonic judgments of

Send Correspondence to: Alfredo Fontanini, Department of Neurobiology and Behavior, Life Science Building Rm 545, SUNY Stony Brook, Stony Brook, NY 11794, alfredo.fontanini@stonybrook.edu, Tel (631) 632-3242, Fax (631) 632-6661.
*CLS and MPHG contributed equally to this work

gustatory stimuli (Ashkenazi and Marks, 2004; Marks and Wheeler, 1998; Nitschke et al., 2006). Similarly, fMRI BOLD responses and patterns of activation in GC differ for expected and unexpected stimuli (Nitschke et al., 2006; Small et al., 2008; Veldhuizen et al., 2007; Veldhuizen et al., 2011). The importance of this phenomenon extends beyond taste. Indeed, in all the sensory modalities expectation biases perception toward anticipated stimuli, thus enhancing stimulus representation (Doherty et al., 2005; Engel et al., 2001; Gilbert and Sigman, 2007; Jaramillo and Zador, 2011; Zelano et al., 2011).

The effects of expectation are not limited to the processing of expected stimuli. Expectation can also modify the background state of sensory networks prior to the presentation of the anticipated stimulus. Changes in pre-stimulus activity are well documented by electrophysiological and imaging studies (Egner et al., 2010; Fontanini and Katz, 2008; Mitchell et al., 2009; Nitschke et al., 2006; O'Doherty et al., 2002; Small et al., 2008; Yoshida and Katz, 2011). Olfactory or verbal cues signaling the availability of tastes result in a general activation of GC (Small et al., 2008; Veldhuizen et al., 2007). Activation of primary sensory cortices by anticipatory cues is also observed at the single neuron level (Kerfoot et al., 2007; Saddoris et al., 2009; Schiltz et al., 2007) and in the temporal patterns of activity preceding the expected stimulus (Engel et al., 2001; Fontanini and Katz, 2008; Mitchell et al., 2009; Womelsdorf et al., 2006). These anticipatory changes in the state of sensory networks are believed to be caused by top-down inputs from higher-order areas (Fontanini and Katz, 2008; Gilbert and Sigman, 2007).

Changes in the background state of sensory networks are thought to play a fundamental role in shaping sensory responsiveness (Arieli et al., 1996; Engel et al., 2001; Fiser et al., 2004; Fontanini and Katz, 2008; Krupa et al., 2004; Poulet and Petersen, 2008). Direct comparison of single neuron coding of expected and unexpected objects revealed changes in cortical responses that could be attributed to modifications of pre-stimulus activity (Krupa et al., 2004; Mitchell et al., 2009; Wiest et al., 2010; Womelsdorf et al., 2006; Yoshida and Katz, 2011). Yet, the mechanisms linking changes in anticipatory activity with the effects of expectation on sensory processing are not fully understood.

Here we study the effects of cue-induced expectation on response dynamics evoked by gustatory stimuli. Single neuron and population responses to unexpected tastants were compared with those evoked by the same, but expected, stimuli. We show that expectation results in rapid coding of stimulus identity and that this phenomenon is mediated by cue-induced anticipatory priming of GC. Simultaneous multi-area recordings and pharmacological manipulations in behaving rats further indicate that the priming effects of anticipatory cues on cortical activity depend on top-down inputs from the basolateral amygdala (BLA), a component of the anticipatory network (Belova et al., 2007; Fontanini et al., 2009; Small et al., 2008) involved in taste coding (Fontanini et al., 2009; Grossman et al., 2008) and with strong connections to GC (Allen et al., 1991).

RESULTS

Single neuron spiking activity was recorded in 20 behaving rats using multiple movable bundles of 16 extracellular electrodes; 9 rats had bilateral GC implants, 4 had bundles in GC and BLA and 7 had recording electrodes in GC and cannulae for intracranial infusion of drugs in BLA. A total of 473 single units were recorded from GC (156 of which pertain to the BLA infusion groups) and 72 from BLA. Subjects were tested after successful training to perform a task designed to study the effects of expectation on gustatory processing. For each trial rats had to wait ~ 40 s after which a tone signaled the availability of a tastant chosen randomly out of four possible (Sucrose, NaCl, Citric Acid or Quinine). The subjects had 3 s to press a lever to self-administer a tastant directly into their mouth via an intra-oral cannula

(IOC) (average latency of lever pressing: 635 ± 228 ms, n = 38). To study expectation in its most general form, only a single tone was used as a cue and no information was given about the identity of the tastant available at each trial. Unexpected tasting was achieved via uncued IOC deliveries of gustatory stimuli presented at random trials and times during the pre-tone period. During each recording session single unit spiking responses to expected self-administered tastants (from here on referred as: ExpT) were compared with responses to the same tastants unexpectedly delivered by the behavioral software (from here on referred as: UT). Each delivery of a tastant was followed, 5 s later, by a water rinse.

Expectation results in faster coding of gustatory information

To begin addressing the effects of expectation on GC sensory responses, the absolute difference between peri-stimulus-time-histograms (ΔPSTH) in response to ExpT and UT was computed and averaged across cells and tastants. This analysis, which provides a measure of the difference between responses to ExpT and UT, showed a striking task-dependency of evoked firing. 58.4 % of the neurons (174/298) produced significantly different firing rate modulations ($p < 0.05$) in the first 2.5 s after stimulus presentation depending on the condition. Figure 1A displays the difference for the first 2.5 s following the presentation of the stimulus. Average ΔPSTH for each tastant follows a similar trend (inset Figure 1A). The largest difference between responses occurred early; ~250 ms after stimulus delivery the difference decayed to 50 % of its maximum (see dotted box, Figure 1A). Firing rates in the first 250 ms significantly differed for 31.2 % (93/298) of GC neurons ($p < 0.05$). No clear trend toward an increase or decrease of firing rates was observed for either condition; the proportion of neurons firing more to UT or to ExpT was similar (See Supp Figure S1 for a complete analysis).

To determine the influence of early changes in firing rates on taste coding, the initial 250 ms were divided in two 125 ms bins. Single neurons were defined as taste responsive in a certain bin if their firing rates in response to the four tastants differed significantly according to a one-way ANOVA ($p < 0.05$). As shown in Figure 1B, the percentage of taste coding neurons was higher for self-deliveries in the first two bins, with the maximal increase, 52.4 %, in the first 125 ms (from 7.04 %, 21/298, for UT to 10.7 %, 32/298, for ExpT) and a 37.8 % increase in the 125–250 ms interval (from 12.4 %, 37/298, for UT to 17.1 %, 51/298, for ExpT). The neurons coding for ExpT were among those being affected by expectation as demonstrated by their ΔPSTH. In those neurons the difference in the first two bins was significantly larger than background values (first 125 ms bin: 7.4 ± 1.1 Hz vs 2.5 ± 0.4 Hz, n = 32, $p < 0.01$; second 125 ms bin: 7.1 ± 0.9 vs 3.1 ± 0.4, n = 51, $p < 0.01$) and larger than the ΔPSTH observed for the other neurons (first 125 ms bin: 3.0 ± 0.3 Hz, n = 266, $p < 0.01$; second 125 ms bin: 2.5 ± 0.2, n = 247, $p < 0.01$).

A classification analysis was used to establish the impact of single cell changes on taste processing in neural ensembles. This analysis made it possible to determine whether ensemble firing patterns in the early portion of responses to ExpT (0–125 ms and 125–250 ms) allowed better stimulus discrimination than responses to UT. Figure 1C shows the result of a population PSTH-based classification algorithm averaged over all of the experimental sessions; a significant difference in favor of ExpT was observed in the first 125 ms (ExpT: 33.8 ± 1.8 %, UT: 27.4 ± 1.9 %, $p < 0.01$, n = 38). While activity evoked by UT did not allow for an above chance performance, responses to ExpT were classified correctly in a significantly larger percentage than chance ($p < 0.01$). Thus, cueing enabled more accurate coding in the earliest response interval. This improvement in taste coding was restricted to the first 125 ms of the response; whereas in the interval between 125 and 250 ms, UT and ExpT trials showed a similar above chance ($p < 0.01$) percent correct (ExpT: 37.5 ± 2.1 %; UT: 37.4 ± 2.1 %, $p = 0.97$). A similar classification was performed after a swapping procedure to determine the contribution of single taste responsive neurons. Responses for

neurons that were taste specific in the first bin of the ExpT condition were swapped with those evoked by UT. The performance for UT significantly increased (32.4 ± 2.1 %, $p < 0.01$) whereas ExpT classification significantly decreased (30.5 ± 1.8 %, $p < 0.05$), making the difference in classification for the two conditions no longer statistically significant ($p = 0.41$). The contribution of taste specific neurons was determinant in mediating the faster onset of stimulus coding.

To further understand the factors determining the improvement in early taste coding, response tuning and trial-to-trial variability were computed. Breadth of tuning was quantified by analyzing the entropy of response profiles (H, see (Smith and Travers, 1979) for its standard application to taste coding) for the neurons mediating the increase in taste coding. Trial-to-trial variability was determined by measuring the average Euclidean distance between single trial population responses for each session (in Figure 1E referred to as dissimilarity index). In the first 125 ms bin the average H value for responses to ExpT showed a small, but significant, decrease relative to that for UT (0.89 ± 0.01 for ExpT and 0.95 ± 0.01 for UT, $p < 0.01$ n = 32; Figure 1D, black trace), indicating that responses to ExpT are more narrowly tuned. In the same bin, population responses for ExpT had a significantly lower trial-to-trial variability (average Euclidean distance: 0.59 ± 0.02 for ExpT and 0.76 ± 0.02 for UT, $p < 0.01$ n = 152 Figure 1E, black trace). Thus, narrowing of tuning and reduction of trial-to-trial variability co-occurred in the first bin. Responses to ExpT in the second 125 ms bin, on the other hand, showed a very small decrease in H (0.87 ± 0.02 for ExpT and 0.90 ± 0.02 for UT, $p < 0.01$ n = 32; Figure 1D, gray trace) and a trending, but no significant increase in the trial-to-trial variability (0.63 ± 0.02 for ExpT and 0.69 ± 0.02 for UT, $p = 0.06$ n = 152, ; Figure 1E, gray trace). Figure 1F displays a representative example of a neuron changing its breadth of tuning in response to ExpT. The histograms on the right detail response profiles in the first 125 ms bin and show a slight sharpening of the tuning in favor of expected sucrose. Figure 1G shows dissimilarity matrices and the corresponding trial-by-trial ensemble responses in the first bin for a representative session, further confirming the differences in trial-to-trial variability in response to UT and ExpT.

Pre-stimulus anticipatory activity correlates with post-stimulus differences

Visual inspection of the representative responses to ExpT in Figure 1F highlights an additional feature of responses to ExpT, the presence of a pre-stimulus ramp in firing rates at the time in which auditory cues are presented (see vertical gray lines). The population PSTH for ExpT (Figure 2A) and the average ΔPSTH (Figure 2B) from 3 s before to 2.5 s after tastant delivery show the generality of this pattern in the dataset. Figure 2A presents a population PSTH computed on a group of 298 neurons and shows a clear ramp in the activity that precedes self-administration of tastants (see also Figure S1). Similarly, the ΔPSTH averaged across trials, neurons and tastants for bins of 125 ms (Figure 2B), provides a striking picture of the relevance of this pre-tastant activity. The average ΔPSTH reached a peak in this last bin before tastant delivery (4.0 ± 0.5 Hz, n = 298) (Figure 2B, see arrowhead "*pre*"); 14.4 % (43/298) of the neurons showed a significant difference in this bin. Pre-stimulus modulations were larger in neurons whose taste evoked activity changed the most. Indeed, the absolute pre-stimulus ΔPSTH, in the last bin before tastant delivery, was significantly ($p < 0.05$) larger for cells with significant post-stimulus ΔPSTH (7.5 ± 1.8 Hz, n = 67) when compared to those that were not modulated by expectation (2.9 ± 0.3 Hz, n = 231). The left panel of Figure 2C shows a significant correlation between pre and post-stimulus differences in firing activity ($r^2 = 0.34$, $p < 0.01$, n = 298). A control comparison between the ΔPSTH for the first post-tastant bin and that for a bin randomly sampled from background activity (represented in Figure 2C, right panel) revealed no correlation ($r^2 = 0.01$, $p = 0.08$), confirming the specificity of the results. Finally, to determine whether

anticipatory activity was present in neurons that improved gustatory classification performance, their pre-tastant ΔPSTH was computed. The presence of firing modulations before gustatory stimulation was confirmed by an average pre-tastant ΔPSTH of 5.7 ± 1.4 Hz, a value significantly larger than that observed in the same cells for spontaneous activity (2.5 ± 0.4 Hz, $p < 0.05$, $n = 32$).

Cue-induced activity: anticipatory priming of cortical neurons—To investigate the relationship between changes in firing activity preceding self-administration and lever pressing, population PSTH for cued and for erroneous lever presses were compared (Figure S2). Erroneous pressing was defined as those uncued, non-tastant delivering lever presses occurring during the foreperiod leading to the cue. While anticipatory activity was present in the population PSTH in response to cued self-administrations, no significant pre-stimulus changes in activity were observed for erroneous lever presses (pre-stimulus activity for erroneous presses was significantly smaller than that for ExpT, $p < 0.01$, $n = 298$). This result points to the importance of predictive cues, and not pressing-related movement, in shaping GC anticipatory activity. The role of auditory cues in triggering anticipatory activity was directly addressed by aligning neural activity to the tone (Figure 3). A total of 26.2 % (78/298) of neurons were found to significantly respond to the cue; of these 19.5 % (58/298) showed excitatory and 6.7 % (20/298) inhibitory responses. The plot in Figure 3A shows the individual PSTH for all the neurons that produced significant cue responses, sorted by the latency of their peak. To verify that cue-responsiveness did not result from conditioned oro-motor responses, we performed multiple control analyses. First, we computed the power spectrum of the firing of cue-responsive neurons. Somatosensory neurons driven by oro-motor behaviors were identified on the basis of a known spectral signature (Katz et al., 2001): a characteristic peak in the 6–9 Hz band (the frequency of licking) in their firing frequency (Figure 3A insets). Only 25.6 % (20/78) of cue-responsive neurons were rhythmically modulated by oro-motor behaviors (black rectangles in the ‘Som’ labeled strip plot in right portion of Figure 3A). These neurons responded to the tone with a significantly ($p < 0.05$) longer latency (90 ± 15 ms, $n = 16$) than those without the somatosensory spectral signature (50 ± 5 ms, $n = 56$). Since this method does not allow for the identification of potential somatosensory neurons that would not show rhythmic responses, a second analysis was performed on high-speed video recordings of the oro-facial region. To determine whether cue responses in neurons without somatosensory rhythmic signature preceded, or followed, mouth movements, the latency of the earliest detectable movement was determined with visual and automated methods in random subsets of sessions (Figures S3 and S6). The average latency of the earliest minimal mouth movements was significantly longer than that of tone responsive neurons that did not have the rhythmic signature (automated methods: 187 ± 27 ms, $p < 0.01$, $n = 10$; blind visual inspection: 248 ± 29 ms, $p < 0.01$, $n = 5$). A session-by-session comparison of neural response and mouth movement latencies triggered by the cue confirmed that responses to cues systematically precede oral movements (Figure S3). This result is further confirmed by the inspection of population PSTH in response to the earliest mouth movements (Figure S3), which shows a pre-movement ramp in firing rates. Thus, a relatively large percentage of recorded GC neurons (19.6 %, 58/298) produce responses to auditory tones that are not secondary to conditioned oral movements. Figure 3B and *C* show population PSTH and representative examples of cue responses in non-rhythmic neurons. To determine whether cue responses depended on learning, we quantified the number of neurons activated by the tone in 6 naïve rats. In the first session in which the tone was introduced only 1 out of 36 neurons recorded produced a non-somatosensory tone response (2.8 % versus 19.5 % after training, $p < 0.05$) with a long latency (99 ms), suggesting that a high incidence of short latency cue-evoked activity could depend on learning and relate to the anticipatory value of the tone (Kerfoot et al., 2007).

If the responses described above are truly anticipatory, they should result from top-down influences. To test this hypothesis we investigated the contribution of BLA, an area of the anticipatory network (Belova et al., 2007; Fontanini et al., 2009; Small et al., 2008) known to send projections to GC (Allen et al., 1991; Saper, 1982) and a possible source of top-down modulation. In a first set of experiments, GC and BLA were simultaneously recorded from rats involved in the task described above. As expected, BLA neurons responded to anticipatory cues (Figure 4A, see also Figure S4 for representative raster plots and PSTH). A total of 20.8 % (15/72) of BLA neurons responded to the tone: 16.6 % (12/72) were excitatory and produced an average response of 19.2 Hz (± 6.4, n = 12), while 4.2 % (3/72) showed inhibition, with firing rates dropping next to 0. The average latency of cue-responsive neurons in BLA was 33 ms (± 3, n = 15), an interval significantly shorter than that observed for GC neurons (49 ± 5 ms, n = 56, $p < 0.01$; Figure 4B). Cross-correlation between BLA spikes and GC local field potentials (LFP) was quantified in the 125 ms following the tone. Figure 4C shows that the average peak in cross-correlation for cue responses significantly exceeded that measured at baseline (0.03 ± 0.006 and 0.02 ± 0.005, n = 10, $p < 0.05$). This correlation values, while small, are consistent with those observed in another study on GC-BLA correlation (Grossman et al., 2008). The difference in latency and the cue dependent strengthening in connectivity are consistent with top-down inputs from BLA neurons driving GC cue-related anticipatory activity. To test the causal role of BLA we recorded cue responses before and after its pharmacological inactivation with the AMPA antagonist NBQX (bilateral injection of 0.2 μl at a concentration of 5 μg/μl). Inactivation of BLA resulted in a significant decrease of the absolute amplitude of peak excitatory responses to cues (from of 13.0 ± 2.8 Hz to 5.8 ± 1.4 Hz after NBQX infusion, $p < 0.05$, n = 5 cue-responsive neurons) (Figure 4D, left panel). No significant difference was observed when saline was injected in BLA (from of 16.4 ± 4.0 Hz to 13.8 ± 3.2 Hz after saline infusion, $p = 0.09$, n = 12 cue-responsive neurons) (Figure 4D, right panel). These results demonstrate that cue responses result from top-down inputs.

Cue-induced activity: pre-play of responses to unexpected tastants—Cue-responsive neurons showed a strong relationship with expectation-induced changes. They had a large average ΔPSTH in the first 125 ms post-tastant, which was significantly higher than that of background activity (6.8 ± 0.9 Hz, versus 3.4 ± 0.5 Hz, n = 58, $p < 0.01$) and significantly exceeded the ΔPSTH for all the other cells (6.8 ± 0.9 Hz, n = 58, versus 2.7 ± 0.3 Hz, n = 240, $p < 0.01$). A large percentage of neurons that coded for ExpT in the first bin were also cue-responsive (39.1 % excluding rhythmic somatosensory neurons; 43.7 % including somatosensory neurons). Visual inspection of the raster plots and PSTH in Figure 3C reveals a striking similarity between the activity following the cue and that triggered by UT (shaded areas). We began analyzing the similarity between cue responses and responses to UT by comparing their trial-to-trial variability. The Fano factor, i.e. the ratio of variance to mean of the spike counts, computed for the first 125 ms of responses in GC (Figure 5A) showed a similar reduction for both gustatory stimuli and auditory cues. Thus, both optimal stimuli (i.e. tastants) and multimodal anticipatory cues (i.e. auditory tones) similarly reduced trial-to-trial variability in GC. To further quantify the extent to which cue responses resembled the initial portion of responses to UT correlation analyses were performed. Responses were computed as firing rates averaged across a period of 125 ms following either the tone or UT. Figure S5A shows the correlation for all the 58 neurons that responded to cues and did not show somatosensory rhythmicity. Neurons in this plot appear to have rather heterogeneous firing rates in response to UT, an indicator of the possible presence of different neuronal classes in our sample (i.e. pyramidal neurons and interneurons). To address this issue we analyzed the width of spike waveforms and spontaneous firing rates for each neuron (Mitchell et al., 2007; Yokota et al., 2011). These two parameters were used to separate putative pyramidal neurons (spike width > 300 μs and

spontaneous firing rates < 10 Hz) from putative interneurons (spike width < 300 μs and spontaneous firing rates > 10 Hz). Neurons with wide spikes and high firing rates or narrow spikes and low firing rates were classified as ambiguous. Figure S5B and C detail the results of these analyses. The population of cue-responsive neurons did indeed contain different classes of neurons. The majority of cue-responsive neurons (70%, 40/58) were putative pyramidal cells (see methods and legend of Figure S5 for more details). We focused all our correlation analyses on this homogeneous sub-population of putative pyramidal neurons. As shown by Figure 5B, firing rates evoked by cues and unexpected tastes were significantly correlated in the population of putative pyramidal neurons (r^2 was 0.38, n = 40, $p < 0.01$). Using the same population as in Figure 5B a running correlation analysis was performed. Trial-averaged running correlation between cue-evoked firing patterns in the first 125 ms and the time course of the UT response (Figure 5C) confirms this result and extends it by showing that the peak of correlation is significantly restricted to the first 125 ms bin of a UT response (0.39, ± 0.02 $p < 0.01$, n = 41). These analyses suggest a strong similarity between the anticipatory patterns evoked by cues and the early activity evoked by uncued, passively delivered gustatory stimuli. A principal component analysis (PCA) based visualization of ensemble dynamics evoked by UT and tones further support this result (Figure 5D), confirming that the cue evokes a state not dissimilar from that evoked by UT in the first 125 ms. The robustness of the results detailed in Figure 5C and D, which were obtained by analyzing only the population of putative pyramidal neurons, was confirmed when the same analyses were performed on the entire population of non-somatosensory cue-responsive neurons (n = 58; Figure S6). No correlation analyses were performed on the group of putative interneurons due to the small sample size.

To determine the impact of cue-dependent activation of GC on the time-course of responses to ExpT, population activity induced by ExpT and UT in putative pyramidal neurons (Figure 6A, gray line and black line respectively) were compared using PCA. The product of this analysis (Figure 6A, B, C) shows that early differences in the response result from the first bin of activity to ExpT (1 gray) moving closer to the second bin evoked by UT (i.e. the time at which taste coding begins; 2 black). The same visualization applied to each tastant (Figure 6B) confirms that the result from the average is general to all stimuli. Responses to ExpT and UT begin to realign 250 ms after delivery of the tastant (Figure 6A, B, C). The running correlation between the first bin of responses to ExpT and the time course of responses to UT confirms the results obtained with PCA (Figure 6D) by showing a broad peak of correlation that similarly involves the first (0–125 ms) and the second (125–250 ms) bin of the responses to UT (0.74 ± 0.01 and 0.72 ± 0.01 respectively, p = 0.22, n = 28). Figure 6E portrays an example of early responses to ExpT resembling later responses to UT. Figure 6 was obtained analyzing the same population of neurons used for Figure 5 (i.e. putative pyramidal neurons, n = 40). Analyses of the entire population of non-somatosensory cue-responsive neurons (n = 58; Figure S6) yielded qualitatively similar results.

Effects of expectation on oro-motor activity—Differences in responses to UT and ExpT could be related to changes in oro-motor activity induced by expectation. To address this issue, an analysis of mouth movements triggered by cues, UT and ExpT was performed. Blind visual inspection and automated image analysis of the oral region were performed for each frame to extract the timing of isolated and rhythmic mouth movements (see methods and Figure S7). Auditory cues produced small mouth movements with an average latency of 189 ± 30 ms (n = 10) and a magnitude that was only 21.4 ± 6.5 % of the amplitude of taste-induced movements. Automated analysis as well as blind visual inspection of video records revealed that cue-evoked mouth movements did not initiate rhythmic mouth movements, which were only evoked by the tastant. The representative single trial and trial-averaged traces from Figure S7 confirm this assessment. The average mouth movement recorded for ExpT revealed only a small ramp before self-administration, which is likely the result of

cue-evoked movements. The amplitude of the mouth movements prior to self-administration is only 12.8 ± 4.7 % of that evoked by ExpT. Tastants, on the other hand, evoked large, rhythmic and long lasting movements. The overall pattern of rhythmic mouth movements was similar for ExpT and UT, as was their amplitude in the first 125 ms (amplitude UT: 104.3 ± 5.4 % of amplitude ExpT). A small, significant difference was observed in their latency: ExpT evoked mouth movements at 66 ± 4 ms, while UT at 96 ± 6 ms. Palatability related behaviors (i.e. tongue protrusions and gapes) also showed differences in the two conditions. In general ExpT evoked more tongue protrusions and less gapes than UT, indicating an expectation-dependent increase of perceived palatability and reduction of aversiveness (Table S1). These type of behaviors occurred at a latency longer than 125 ms (Figure 2A and B, Figure S1, and Table S1).

DISCUSSION

The results presented here demonstrate the effects of cue-triggered expectation on temporal processing of gustatory stimuli in alert animals and describe cortical and amygdalar anticipatory signals responsible for this modulation.

Analysis of temporal dynamics of spiking responses in GC revealed that expectation effects were maximal in the early portion of the response. Early changes in firing rates evoked by ExpT resulted in more rapid coding of gustatory information. This effect was mediated by an increase in the number of neurons that were selective for expected tastants, by a sharpening of their tuning and by a reduction of trial-to-trial variability in ensemble responses. These changes were related to anticipatory modifications of the cortical state triggered by the associative cue prior to gustatory stimulation. Cues predicting the availability of gustatory stimuli dramatically altered the activity of GC neurons. Multiple lines of evidence confirmed that cue responses in GC were not secondary to mouth movements. Instead, they appeared to emerge with learning and were the result of top-down inputs from BLA, a hub of anticipatory signals known to project to GC. Further analysis of responses from putative pyramidal neurons unveiled a strong correlation between cue-evoked responses and activity triggered by UT. Similarly to early activity evoked by UT, which is not specific to the chemical identity of the stimulus, cue-evoked responses acted by priming cortical circuits. The presence of the anticipatory priming before delivery of ExpT allowed GC to “save” time and more readily encode expected tastants. While no analysis of the correlation patterns was performed on interneurons (due to the small sample size), the same analyses applied to the entire population of cue-responsive neurons yielded similar results.

Task dependency of response dynamics

Gustatory cortical neurons process taste-related information via dynamic modulations of firing activity (Gutierrez et al., 2010; Jones et al., 2006; Katz et al., 2002; Stapleton et al., 2006). Three temporal windows, each coding different aspects of gustatory experience, have been classically described in the time course of responses to UT delivered via IOC (Fontanini and Katz, 2006; Grossman et al., 2008; Katz et al., 2002). Early reports showed that the initial portion of a response, i.e. from 0 to ~250 ms following taste stimulation, is devoted to processing the arrival of a fluid in the mouth with little coding of its chemical identity. By comparing response dynamics to ExpT and UT delivered via IOC, we showed that the temporal structure of the coding scheme can be altered by expectation. Taste coding can occur rapidly if tastants are expected. This improvement occurs due to a sharpening of response tuning combined with a decrease in the trial-to-trial variability of ensemble responses in the first 125 ms. The decrease in breadth of tuning was small, but it reached levels comparable with those observed for responses in the second bin. However, sharpening of tuning alone could not entirely explain our results as it also occurred for responses to

ExpT in the second bin, a period in which classification performance does not change. Reduction of response variability, known to also occur in the visual system during an attentional task (Mitchell et al., 2009), appears critical to explain differences in classification performance between the first and second bin. Indeed, the absence of reduction in trial-to-trial variability for responses to ExpT in the second bin correlates with the lack of difference in classification performance.

These results show that in alert animals GC does not need to rely on a small subset of narrowly tuned neurons (Chen et al., 2011) to discriminate gustatory information. Instead, taste processing can be successfully achieved via broadly tuned neurons, distributed around much of GC, and whose selectivity and reliability are dynamically modulated by the behavioral state of the subject. Beyond taste, our data emphasize the importance of behavioral state in sculpting sensory processing and provide evidence for task-dependent multiplexing of temporal coding (Fontanini and Katz, 2008; Gilbert and Sigman, 2007). According to this view, the content and the timing of sensory codes are determined not only by the physical-chemical structure of stimuli and by the timing of their presentation, but also by the demands of the task in which the animal is involved. These conclusions can be extrapolated to the interpretation of behavioral results on stimulus discrimination latencies and reaction times, which also vary depending on the behavioral state of the subject (Fontanini and Katz, 2006; Jaramillo and Zador, 2011; Womelsdorf et al., 2006).

Relationship between the effects of expectation and motor responses

Multiple analyses were performed to exclude the possibility that the effects of expectation were secondary to movement. The changes in the background state of GC prior to ExpT were not related to lever pressing movement. Erroneous lever pressing in the absence of the cue had no effect on background firing rates, pointing to the cue as the key trigger of anticipatory activity. Cue-evoked changes in firing rates were only minimally related to rhythmic mouth movement. Indeed, most of the neurons that responded to cues did not show the characteristic rhythmic firing associated with licking. Neurons with licking-related rhythmicity were excluded from further analysis. Latency analyses on non-rhythmic neurons revealed that cue responses had fast onset, significantly faster than mouth movements. In fact, responses to anticipatory tones appeared well before any visible mouth movement could be observed. We cannot exclude the possibility that small tongue movements could have occurred in the mouth without any visible movement of the oral region, however the disappearance of cue responses following BLA inactivation strongly supports the cognitive nature of cue-related activity in GC. While anticipatory mouth movements were not the cause of cue responses, they could in theory contribute to the difference between responses to UT and ExpT. Analysis of visible mouth movements immediately preceding ExpT revealed only minor activity. Movements were triggered by the cue and decreased before self-delivery. Large, rhythmic movements, likely related to licking (Travers and Jackson, 1992; Travers et al., 1986), were only observed following the delivery of tastants. ExpT and UT evoked movements with similar amplitude, but with different latencies. Masticatory responses to ExpT and UT occurred ~66 ms and ~95 ms respectively, in both cases within the first 125 ms from stimulus delivery. The faster onset of mouth movements after ExpT is consistent with attentional and anticipatory effects on reaction times (Jaramillo and Zador, 2011; Womelsdorf et al., 2006) and might in part contribute to the differences in stimulus processing. Indeed, the small, but significant, difference in latency of mouth movements suggests a possible coupling between cognitive and sensorimotor processes in mediating the effects of expectation.

Finally, we quantified the occurrence of palatability-related oro-facial reactions (i.e. small tongue protrusions, lateral tongue protrusions and gapes). Expected tastants appeared to be more palatable and less aversive than unexpected stimuli, a phenomenon observed also after

learning (Spector et al., 1988), after alterations of sodium homeostasis (Tindell et al., 2006) and after changes in the state of arousal (Fontanini and Katz, 2006). An analysis of the latency of oro-facial reactions revealed that these behaviors occur well-after the onset of rapid coding, a result in general agreement with the literature (Tindell et al., 2006; Travers and Norgren, 1986). The latency of oro-facial reactions appeared only partially affected by expectation. Small tongue protrusions had a significantly faster onset when evoked by ExpT; latency of gapes and lateral tongue protrusions did not appear to be modulated by expectation. While overall differences in orofacial reactivity occur too late to influence the changes in neural activity observed in the first 125 ms bin, they suggest interesting effects of expectation on the processing of palatability.

Role of BLA in mediating expectation-related changes

A fundamental issue addressed here is that of the sources of expectation-related signals. Experiments in both humans and animal models point to BLA as a key area in processing anticipatory cues, expectation and taste (Belova et al., 2007; Fontanini et al., 2009; Roesch et al., 2010). BLA, one of the several areas activated by expectation with anatomical projections to GC (Allen et al., 1991), exerts excitatory and inhibitory effects (Ferreira et al., 2005; Hanamori, 2009; Yamamoto et al., 1984). Recent *in vivo* intracellular recordings showing the ability of BLA inputs to promote spiking in GC neurons further strengthen the functional relevance of this connection (Stone et al., 2011). Our results indicate that BLA can have a crucial role in directly promoting cue responses in GC. Interactions between frontal circuits and amygdala are responsible for the emergence of cue responses in BLA (Schoenbaum and Roesch, 2005), which would then transfer this signal to GC.

As for the psychological nature of the signal provided by BLA, the recent suggestions that BLA might be involved in processing saliency, attention and expectation (Balleine and Killcross, 2006; Holland and Gallagher, 1999; Roesch et al., 2010) are entirely consistent with our results. The priming of GC networks induced by cues could be related to a salient anticipatory signal reaching sensory cortices via BLA. Our results, thus, extend the involvement of BLA in stimulus processing beyond its role of enriching sensory codes with emotional value (Fontanini et al., 2009; Grossman et al., 2008; Maren et al., 2001) and point at a more dynamic and context-dependent relationship between amygdala and sensory processing .

General and specific expectation

Sensory perception in general, and taste perception in particular, are heavily influenced by expectation. Most of the studies on the subject have focused on a very specific form of expectation, which involves the anticipatory knowledge of the identity of the stimulus. fMRI and immediate early gene studies have shown that this form of expectation results in the anticipatory activation of stimulus-specific representations (Nitschke et al., 2006; Saddoris et al., 2009; Zelano et al., 2011). In this study we address the most general form of expectation, that of a stimulus occurring in a specific modality regardless of its specific identity. We showed that cues can associatively activate GC even when specific information about the identity of the gustatory stimulus is not available. This anticipatory activation is remarkably similar to general patterns that prime GC following the presentation of UT. We further explained the mechanism through which this anticipatory priming can influence taste coding. Our results can be extrapolated to the case of specific expectation. Indeed it is likely that cues associated with specific stimuli would not only produce patterns of activity correlated with those evoked by the sensory dimensions they predict (Kerfoot et al., 2007; Saddoris et al., 2009), but also result in the dynamic modulation of sensory responses to the expected dimensions.

EXPERIMENTAL PROCEDURES

Experimental subjects

All the experimental procedures were performed according to federal, state and university regulations. Female Long Evans rats (275–350 g) served as the subjects in this study. Animals were maintained on a 12h/12h light/dark schedule and were given *ad libitum* access to chow and water, unless otherwise specified.

Surgery

See supplemental material for surgical procedures and details on the implantation of electrodes and cannulae in GC and BLA and post-operative recovery.

Behavioral training

After the recovery time, rats were started on a water-restriction regimen (45 min of water/day). After they were habituated to restraint conditions and to receiving fluids through IOC, subjects were progressively trained to wait for a period of at least 40 ± 3 s (ITI) and to press the lever at the onset of a 75 dB auditory tone. Rats had to press within 3 s after the tone to collect the fluid; after the lever press (or 3 s), the tone stopped and a new trial was started. Early presses were discouraged by the addition of a 2 s delay of the cue. During experimental sessions additional tastants were unexpectedly delivered (UT) at random times near the middle of the ITI, at random trials and in the absence of the anticipatory cue. Expected, self-administered and UT were selected randomly. After the end of each experimental session, electrodes were moved at least 150 μm.

Stimulus delivery

Four basic tastants (100 mM NaCl, 100 mM sucrose, 100 mM citric acid, and 1 mM quinine HCl) were delivered through a manifold of 4 polyimide tubes slid into the IOC (Fontanini et al., 2009). Computer-controlled solenoid valves pressure ejected ~40 μl of fluids (opening time: ~40 ms) directly into the mouth. 50 μl of water were delivered as a rinse through a second IOC 5 s after the delivery of each tastant. Each tastant was delivered for at least 6 trials in each condition.

Electrophysiological and video recordings

Single neuron action potentials and LFP were simultaneously amplified, bandpass filtered (at 300-8K Hz for single units and 3 to 90 Hz for LFP), digitized and recorded to a computer (Plexon, Dallas, TX). Single units of at least 3:1 signal-to-noise ratio were isolated using a template algorithm, cluster cutting techniques and examination of inter-spike interval plots (Offline Sorter, Plexon, Dallas, TX). Oro-facial reactions were video recorded and videos were synchronized with electrophysiological recordings

BLA inactivation procedures

Rats implanted with injection cannulae were trained to perform the cued, self-administration paradigm. Once the rats were successfully trained, experimental sessions began. A total of 26 sessions were performed on 7 rats. Each session was divided into two sections: a pre-NBQX infusion and post-NBQX infusion portion. See supplemental material for additional details on the experimental protocol.

Analysis of electrophysiological data

Spike sorting and data analysis were performed using Offline Sorter, Neuroexplorer (Plexon Inc) and MATLAB (Mathworks, Natick MA).

Taste responsiveness—Single neuron and population PSTH were compiled around deliveries of tastants. Unless otherwise specified in the text, a bin size of 125 ms was used. The analyses were repeated using different bin width and yielded similar results. Neurons were defined as taste-responsive within each bin if the firing rates evoked by the four stimuli significantly differed from each other with a p value < 0.05 using a one-way ANOVA (trials × tastants). The breadth of tuning of each neuron in each bin was quantified by measuring entropy (H). H was computed as previously reported (Smith and Travers, 1979) using the following formula:

$$H = -K\sum_{i=1}^{n} Pi \log Pi$$

where K is a constant and P_i is the proportional response to each tastant. Low H indicated higher tastant selectivity of a response, whereas high H represented broader tuning (H = 1 means that the neuron responds to all the stimuli in the same way). Consistent with prior literature in the taste field, we performed entropy analysis on each neuron's average response profile hence individual neuron H values yielded no confidence interval. Single trial classification analysis was performed for each ensemble of simultaneously recorded neurons on the basis of their PSTH (Jones et al., 2007). A vector of firing rates was computed for each group of neurons and in each bin. Single trials were classified by comparing their population response with the average population responses for each of the four tastants. Average population responses were compiled using all the trials minus the one being classified. The Euclidean distance between the single trial population vector of firing rates and the average response was used to measure the similarity. This analysis held a percent correct classification for each bin in a session. Classification performance was then averaged across all the sessions and differences between conditions for each bin were compared across conditions using a t-test ($p < 0.05$).

Cue-responsiveness—Analysis of cue responses was limited to the window from the onset of the cue to the time of the earliest lever press for each session. Responses to cues were considered significant when the comparison of post-cue with spontaneous firing averaged across 50 ms wide bins produced a $p < 0.05$ with one-way ANOVA and Tukey-Kramer *post-hoc* analyses. As with taste responses, overall responsiveness to cues was visualized relying on population PSTH averaged across multiple neurons. The latency of tone responses was computed using analyses techniques based on the cumulative sum of spiking responses across trials (Wiest et al., 2005). Briefly, for each neuron all the trials were combined and binned at 1 ms. The cumulative sum of spike counts was then calculated from 500 ms before the cue to the time of the first lever press after the tone. Expected cumulative sum was computed on the basis of the pre-stimulus firing rate. Deviations of the actual cumulative sum from the expected one were determined for each bin. The first of 3 consecutive post-stimulus bins larger than two times the standard deviation was considered the onset of the tone response. Results were validated by blind inspection (neurons yielding conflicting results were dropped to avoid distortion of the average). To determine the subset of neurons that were modulated by mouth movements, the frequency profile of spontaneous spiking activity was determined using power spectral analysis (Katz et al., 2001). The power spectrum of the firing for each neuron was computed in the band between 0.5 and 50 Hz on the basis of a smoothed FFT with frequency resolution of ~ 0.2 Hz. A peak in the licking frequency (5–9 Hz) characterized somatosensory neurons. Comparison of latencies of tone responses between somatosensory and non-somatosensory GC neurons and between the latter and BLA cue responses was performed using paired t-test. Significance of the difference between cue response onsets and latency of earliest mouth movements was

assessed relying on a t-test. To further assess the temporal relationship between cue responses and onset of mouth movements, raster plots, single neuron PSTH and population PSTH were compiled.

Response variability—Trial-to-trial variability of population responses was computed on the basis of neural ensembles recorded in each session. For each tastant, trial and 125 ms wide bin a population vector of firing rates was computed. Each population vector was normalized to the peak firing rate within the vector; this procedure allowed us to extract for each trial an across-neurons activation pattern independent of peak firing rates. Pair-wise Euclidean distance between all the trials was averaged and used to assess trial-to-trial dissimilarity index and plot dissimilarity matrices. Dissimilarity indices for all the bins and tastes were compared for ExpT and UT using a t-test. Single neuron trial-to-trial variability of spontaneous activity and responses to the cue and passive tastants was computed for each bin by measuring the ratio of the variance to the mean of spike counts across trials (Fano factor: (Churchland et al., 2010; Mitchell et al., 2009)). Fano factors for all the cue-responsive neurons that had an excitatory response and did not show somatosensory rhythmicity were averaged and compared using a t-test.

Identification of different cell classes—See supplemental material.

Differences between responses to ExpT and UT—Firing rate differences between responses to ExpT and UT were quantified by subtraction for each time bin ($\Delta PSTH = PSTH_{ExpT} - PSTH_{UT}$). ΔPSTH were performed on PSTH having either 50 or 125 ms wide bins. Negative values indicated larger firing rates for ExpT; both negative and positive values were used for linear regression analysis. To analyze and visualize the net difference between the two conditions, the absolute value of the ΔPSTH was used and averaged for all the neurons. Significance of the ΔPSTH at a specific time point was assessed using paired t-test to compare it with background ΔPSTH. The number of neurons that produced significantly different tastant responses in the two conditions was assessed by using a two-way-ANOVA ([expected/unexpected trials]x tastants) on either single bins or on responses averaged across 2.5 s. Correlation between ΔPSTH before and after gustatory stimulation was established performing a linear regression analysis. ΔPSTH for the last 125 ms before stimulus and for the first 125 after stimulus were used. This analysis was performed on all the neurons in which UT and ExpT were compared.

Correlation between responses—Correlation was established via linear regression analysis of single cell firing rates evoked by either UT or tones over a period of 125 ms from the stimulus. In few sessions (i.e. when pressing occurred before 125 ms) cue responses could be measured only over an interval shorter than 125 ms. In this case, responses to cues were measured from the onset of the tone to the time of the earliest lever press. Responses to UT were computed over a same length interval. Firing rates were normalized to background firing. All the cue-responsive neurons with no somatosensory rhythmicity were used for the correlation analysis. K-means clustering of cue and UT responses in this population suggested the presence of two sub-groups with different firing rates. To examine how a single bin of population activity (i.e. the first 125 ms after either the cue or self-administrations) correlated with the whole time course of responses in another condition a running-correlation was used. Activity at each time point was described by a population vector of firing rates for all the cells that were cue-responsive and that fired to tastants with less than 30 Hz above background. Population activity in the reference bin was correlated with that in each bin composing the time course of the target response from 1 s before to 2.5 after presentation of UT. The correlation was performed across single trials and averaged.

The significance of peaks and differences was established with a one-way ANOVA and a Tukey-Kramer *post-hoc* test.

Visualization of trajectories—To visualize the time course of population activity as a trajectory in space, a PCA was used. PCA was performed for responses to cues, UT and ExpT. PCA was applied on 2-D matrices composed by the trial-averaged activity for the population of neurons versus each 125 ms time bin ([neurons × time]). Tastant responses went from −2 s to 2.5 s after stimulus presentation, while cue responses were limited to an interval going from −2 s to 125 ms after the tone. The difference between the Euclidean distance for homologous bins in different conditions (i.e. bin1 ExpT and bin1 UT; bin2 ExpT and bin2 UT, etc) and that for successive bins in different conditions (i.e. bin1 ExpT and bin2 UT; bin2 ExpT and bin3 UT, etc) was used to verify time course of the similarity between bins. Negative values indicated that the distance for successive bins was shorter than that for homologues bins, i.e. that bin1 ExpT was more similar to bin2 UT than bin1 UT.

Spike-field correlation—The correlation analysis between spiking in BLA cue-responsive neurons and LFP from GC was measured for a 125 ms wide bin either preceding (control) or following the onset of the tone. Eight, simultaneously recorded GC LFP were used for each cell. The cross-correlation was computed on a trial-to-trial basis between the continuous LFP and the rate histogram using a bin size of 1 ms. The average cross-correlogram was computed for each cell-LFP pairing. To eliminate the influence from stimulus-induced covariation, a cross-correlogram was performed on pairs of signals coming from different trials (trial-shuffle) and was subtracted from the average cross-correlogram on same trials. The peak occurring within a ±50 ms lag of the resulting cross-correlogram was measured for both pre and post tone segments and the values compared with a t-test.

Analysis of mouth movements and oro-facial behaviors

See supplemental material.

Histology

See supplemental material.

Supplementary Material

Refer to Web version on PubMed Central for supplementary material.

Acknowledgments

The authors would like to thank Dr. Craig Evinger, Dr. Ahmad Jezzini, Dr. Giancarlo La Camera, Dr. Lorna Role, Haixin Liu and Martha Stone for the very helpful comments and discussions. AF would like to add a special acknowledgement to Drs. Don Katz and Arianna Maffei for their always insightful feedback. This work was supported by National institute of Deafness and Other Communication Disorders Grants R01-DC010389, R03-DC008885 and by a Klingenstein Foundation Fellowship (AF).

References

Allen GV, Saper CB, Hurley KM, Cechetto DF. Organization of visceral and limbic connections in the insular cortex of the rat. J Comp Neurol. 1991; 311:1–16. [PubMed: 1719041]

Arieli A, Sterkin A, Grinvald A, Aertsen A. Dynamics of ongoing activity: explanation of the large variability in evoked cortical responses. Science. 1996; 273:1868–1871. [PubMed: 8791593]

Ashkenazi A, Marks LE. Effect of endogenous attention on detection of weak gustatory and olfactory flavors. Percept Psychophys. 2004; 66:596–608. [PubMed: 15311659]

Balleine BW, Killcross S. Parallel incentive processing: an integrated view of amygdala function. Trends Neurosci. 2006; 29:272–279. [PubMed: 16545468]

Belova MA, Paton JJ, Morrison SE, Salzman CD. Expectation modulates neural responses to pleasant and aversive stimuli in primate amygdala. Neuron. 2007; 55:970–984. [PubMed: 17880899]

Chen X, Gabitto M, Peng Y, Ryba NJ, Zuker CS. A gustotopic map of taste qualities in the mammalian brain. Science. 2011; 333:1262–1266. [PubMed: 21885776]

Churchland MM, Yu BM, Cunningham JP, Sugrue LP, Cohen MR, Corrado GS, Newsome WT, Clark AM, Hosseini P, Scott BB, et al. Stimulus onset quenches neural variability: a widespread cortical phenomenon. Nat Neurosci. 2010; 13:369–378. [PubMed: 20173745]

Doherty JR, Rao A, Mesulam MM, Nobre AC. Synergistic effect of combined temporal and spatial expectations on visual attention. J Neurosci. 2005; 25:8259–8266. [PubMed: 16148233]

Egner T, Monti JM, Summerfield C. Expectation and surprise determine neural population responses in the ventral visual stream. J Neurosci. 2010; 30:16601–16608. [PubMed: 21147999]

Engel AK, Fries P, Singer W. Dynamic predictions: oscillations and synchrony in top-down processing. Nat Rev Neurosci. 2001; 2:704–716. [PubMed: 11584308]

Ferreira G, Miranda MI, De la Cruz V, Rodriguez-Ortiz CJ, Bermudez-Rattoni F. Basolateral amygdala glutamatergic activation enhances taste aversion through NMDA receptor activation in the insular cortex. Eur J Neurosci. 2005; 22:2596–2604. [PubMed: 16307602]

Fiser J, Chiu C, Weliky M. Small modulation of ongoing cortical dynamics by sensory input during natural vision. Nature. 2004; 431:573–578. [PubMed: 15457262]

Fontanini A, Grossman SE, Figueroa JA, Katz DB. Distinct subtypes of basolateral amygdala taste neurons reflect palatability and reward. J Neurosci. 2009; 29:2486–2495. [PubMed: 19244523]

Fontanini A, Katz DB. State-dependent modulation of time-varying gustatory responses. J Neurophysiol. 2006; 96:3183–3193. [PubMed: 16928791]

Fontanini A, Katz DB. Behavioral states, network states, and sensory response variability. J Neurophysiol. 2008; 100:1160–1168. [PubMed: 18614753]

Gilbert CD, Sigman M. Brain states: top-down influences in sensory processing. Neuron. 2007; 54:677–696. [PubMed: 17553419]

Grossman SE, Fontanini A, Wieskopf JS, Katz DB. Learning-related plasticity of temporal coding in simultaneously recorded amygdala-cortical ensembles. J Neurosci. 2008; 28:2864–2873. [PubMed: 18337417]

Gutierrez R, Simon SA, Nicolelis MA. Licking-induced synchrony in the taste-reward circuit improves cue discrimination during learning. J Neurosci. 2010; 30:287–303. [PubMed: 20053910]

Hanamori T. Effects of electrical and chemical stimulation of the amygdala on the spontaneous discharge in the insular cortex in rats. Brain Res. 2009; 1276:91–102. [PubMed: 19389389]

Holland PC, Gallagher M. Amygdala circuitry in attentional and representational processes. Trends Cogn Sci. 1999; 3:65–73. [PubMed: 10234229]

Jaramillo S, Zador AM. The auditory cortex mediates the perceptual effects of acoustic temporal expectation. Nat Neurosci. 2011; 14:246–251. [PubMed: 21170056]

Jones LM, Fontanini A, Katz DB. Gustatory processing: a dynamic systems approach. Curr Opin Neurobiol. 2006; 16:420–428. [PubMed: 16842991]

Jones LM, Fontanini A, Sadacca BF, Miller P, Katz DB. Natural stimuli evoke dynamic sequences of states in sensory cortical ensembles. Proc Natl Acad Sci U S A. 2007; 104:18772–18777. [PubMed: 18000059]

Katz DB, Nicolelis MA, Simon SA. Gustatory processing is dynamic and distributed. Curr Opin Neurobiol. 2002; 12:448–454. [PubMed: 12139994]

Katz DB, Simon SA, Nicolelis MA. Dynamic and multimodal responses of gustatory cortical neurons in awake rats. J Neurosci. 2001; 21:4478–4489. [PubMed: 11404435]

Kerfoot EC, Agarwal I, Lee HJ, Holland PC. Control of appetitive and aversive taste-reactivity responses by an auditory conditioned stimulus in a devaluation task: a FOS and behavioral analysis. Learn Mem. 2007; 14:581–589. [PubMed: 17761543]

Krupa DJ, Wiest MC, Shuler MG, Laubach M, Nicolelis MA. Layer-specific somatosensory cortical activation during active tactile discrimination. Science. 2004; 304:1989–1992. [PubMed: 15218154]

Maren S, Yap SA, Goosens KA. The amygdala is essential for the development of neuronal plasticity in the medial geniculate nucleus during auditory fear conditioning in rats. J Neurosci. 2001; 21:RC135. [PubMed: 11245704]

Marks LE, Wheeler ME. Focused attention and the detectability of weak gustatory stimuli. Empirical measurement and computer simulations. Ann N Y Acad Sci. 1998; 855:645–647. [PubMed: 9929665]

Mitchell JF, Sundberg KA, Reynolds JH. Differential attention-dependent response modulation across cell classes in macaque visual area V4. Neuron. 2007; 55:131–141. [PubMed: 17610822]

Mitchell JF, Sundberg KA, Reynolds JH. Spatial attention decorrelates intrinsic activity fluctuations in macaque area V4. Neuron. 2009; 63:879–888. [PubMed: 19778515]

Nitschke JB, Dixon GE, Sarinopoulos I, Short SJ, Cohen JD, Smith EE, Kosslyn SM, Rose RM, Davidson RJ. Altering expectancy dampens neural response to aversive taste in primary taste cortex. Nat Neurosci. 2006; 9:435–442. [PubMed: 16462735]

O'Doherty JP, Deichmann R, Critchley HD, Dolan RJ. Neural responses during anticipation of a primary taste reward. Neuron. 2002; 33:815–826. [PubMed: 11879657]

Poulet JF, Petersen CC. Internal brain state regulates membrane potential synchrony in barrel cortex of behaving mice. Nature. 2008; 454:881–885. [PubMed: 18633351]

Roesch MR, Calu DJ, Esber GR, Schoenbaum G. All that glitters ... dissociating attention and outcome expectancy from prediction errors signals. J Neurophysiol. 2010; 104:587–595. [PubMed: 20554849]

Saddoris MP, Holland PC, Gallagher M. Associatively learned representations of taste outcomes activate taste-encoding neural ensembles in gustatory cortex. J Neurosci. 2009; 29:15386–15396. [PubMed: 20007463]

Saper CB. Convergence of autonomic and limbic connections in the insular cortex of the rat. J Comp Neurol. 1982; 210:163–173. [PubMed: 7130477]

Schiltz CA, Bremer QZ, Landry CF, Kelley AE. Food-associated cues alter forebrain functional connectivity as assessed with immediate early gene and proenkephalin expression. BMC Biol. 2007; 5:16. [PubMed: 17462082]

Schoenbaum G, Roesch M. Orbitofrontal cortex, associative learning, and expectancies. Neuron. 2005; 47:633–636. [PubMed: 16129393]

Small DM, Veldhuizen MG, Felsted J, Mak YE, McGlone F. Separable substrates for anticipatory and consummatory food chemosensation. Neuron. 2008; 57:786–797. [PubMed: 18341997]

Smith DV, Travers JB. A metric for the breadth of tuning of gustatory neurons. Chemical Senses. 1979; 4:215–229.

Spector AC, Breslin P, Grill HJ. Taste reactivity as a dependent measure of the rapid formation of conditioned taste aversion: a tool for the neural analysis of taste-visceral associations. Behav Neurosci. 1988; 102:942–952. [PubMed: 2850815]

Stapleton JR, Lavine ML, Wolpert RL, Nicolelis MA, Simon SA. Rapid taste responses in the gustatory cortex during licking. J Neurosci. 2006; 26:4126–4138. [PubMed: 16611830]

Stone ME, Maffei A, Fontanini A. Amygdala stimulation evokes time-varying synaptic responses in the gustatory cortex of anesthetized rats. Front Integr Neurosci. 2011; 5:3. [PubMed: 21503144]

Tindell AJ, Smith KS, Pecina S, Berridge KC, Aldridge JW. Ventral pallidum firing codes hedonic reward: when a bad taste turns good. J Neurophysiol. 2006; 96:2399–2409. [PubMed: 16885520]

Travers JB, Jackson LM. Hypoglossal neural activity during licking and swallowing in the awake rat. J Neurophysiol. 1992; 67:1171–1184. [PubMed: 1597706]

Travers JB, Norgren R. Electromyographic analysis of the ingestion and rejection of sapid stimuli in the rat. Behav Neurosci. 1986; 100:544–555. [PubMed: 3741605]

Travers SP, Pfaffmann C, Norgren R. Convergence of lingual and palatal gustatory neural activity in the nucleus of the solitary tract. Brain Res. 1986; 365:305–320. [PubMed: 3947995]

Veldhuizen MG, Bender G, Constable RT, Small DM. Trying to detect taste in a tasteless solution: modulation of early gustatory cortex by attention to taste. Chem Senses. 2007; 32:569–581. [PubMed: 17495173]

Veldhuizen MG, Douglas D, Aschenbrenner K, Gitelman DR, Small DM. The Anterior Insular Cortex Represents Breaches of Taste Identity Expectation. J Neurosci. 2011; 31:14735–14744. [PubMed: 21994389]

Wiest MC, Bentley N, Nicolelis MA. Heterogeneous integration of bilateral whisker signals by neurons in primary somatosensory cortex of awake rats. J Neurophysiol. 2005; 93:2966–2973. [PubMed: 15563555]

Wiest MC, Thomson E, Pantoja J, Nicolelis MA. Changes in S1 neural responses during tactile discrimination learning. J Neurophysiol. 2010; 104:300–312. [PubMed: 20445033]

Womelsdorf T, Fries P, Mitra PP, Desimone R. Gamma-band synchronization in visual cortex predicts speed of change detection. Nature. 2006; 439:733–736. [PubMed: 16372022]

Yamamoto T, Azuma S, Kawamura Y. Functional relations between the cortical gustatory area and the amygdala: electrophysiological and behavioral studies in rats. Exp Brain Res. 1984; 56:23–31. [PubMed: 6468568]

Yokota T, Eguchi K, Hiraba K. Functional properties of putative pyramidal neurons and inhibitory interneurons in the rat gustatory cortex. Cereb Cortex. 2011; 21:597–606. [PubMed: 20615912]

Yoshida T, Katz DB. Control of prestimulus activity related to improved sensory coding within a discrimination task. J Neurosci. 2011; 31:4101–4112. [PubMed: 21411651]

Zelano C, Mohanty A, Gottfried JA. Olfactory predictive codes and stimulus templates in piriform cortex. Neuron. 2011; 72:178–187. [PubMed: 21982378]

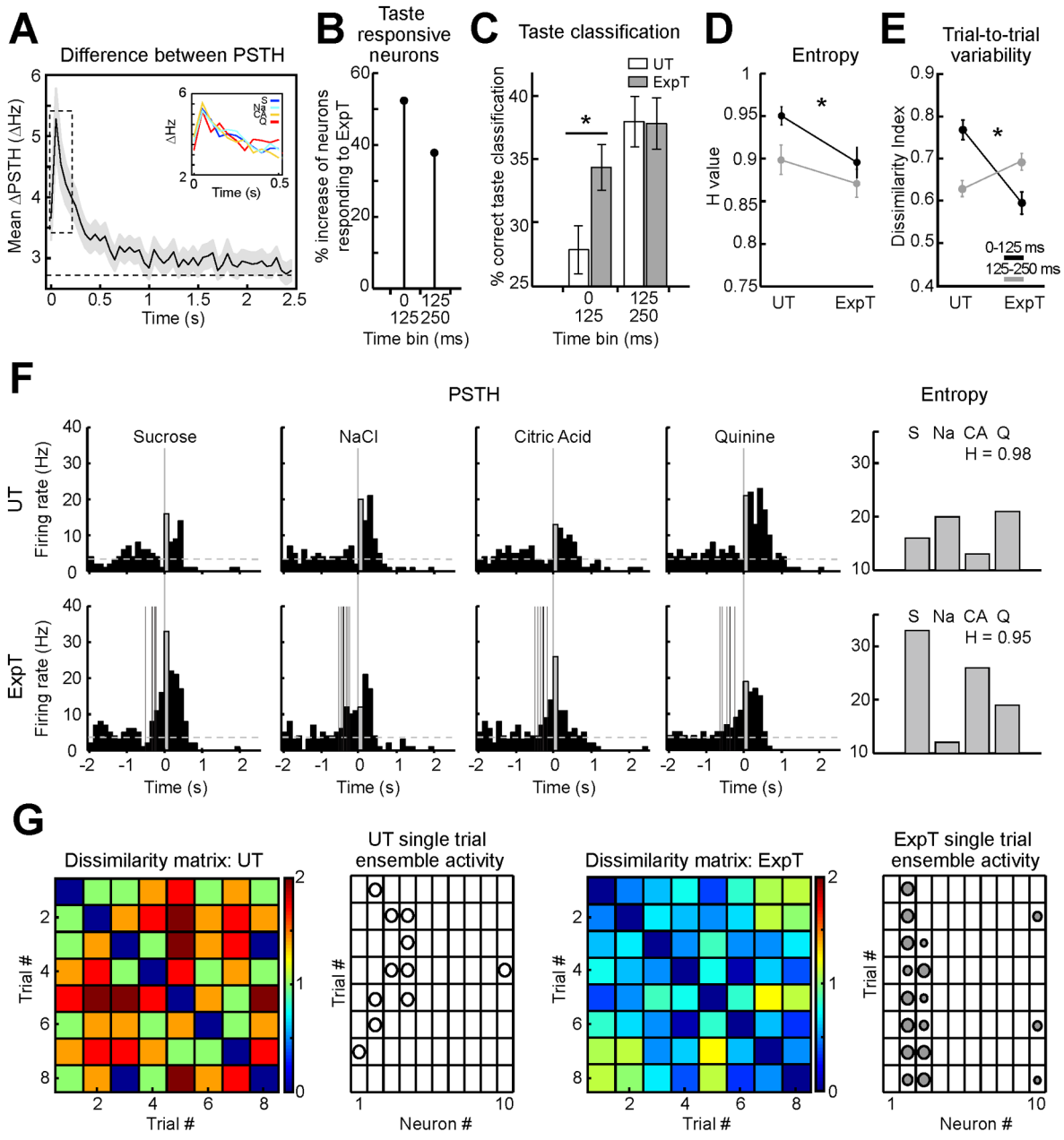

Figure 1.

General expectation promotes rapid coding of gustatory information. **A.** ΔPSTH in response to ExpT and UT (n = 298 neurons). The average ΔPSTH (bin width = 50 ms) is maximal in the first 250 ms (dotted box) following gustatory stimulation (t = 0). Shading around the solid black line represents the standard error of the mean (SEM). The dashed line is the average ΔPSTH for spontaneous activity measured over 2 s before the onset of the cue. Inset: ΔPSTH for each tastant (S = Sucrose, blue; Na = NaCl, cyan; CA = Citric Acid, orange and Q = quinine, red). **B.** Percentage increase in the number of neurons coding for ExpT relative to UT during the first two 125 ms bins following stimulus presentation. **C.** Taste classification of single trials in response to UT and ExpT. The bars in the histogram (white: UT; gray: ExpT) represent the percentage of trials that were correctly classified as S, NaCl, CA or Q on the basis of their population activity in the first and second bin.

Performance for ExpT significantly exceeded that for UT in the first bin. Black asterisk: significant difference. **D.** Entropy (H) value of response profiles. Entropy is significantly smaller for ExpT than UT in both the bins. The black asterisk indicates significant differences between UT and ExpT for the first bin. **E.** Trial-to-trial variability for responses to UT and ExpT. The plot details the pairwise Euclidean distance between single trial ensemble responses (i.e. dissimilarity index). Trial-to-trial variability is significantly smaller for ExpT than for UT only in the first 125 ms. Black line: 0–125 ms bin; gray line: 125–250 ms bin. The black asterisk indicates significant differences between UT and ExpT for the first bin. **F.** PSTH of a representative neuron in response to UT (top) and ExpT (bottom) (tastant delivery is at t = 0). Gray bars represent the activity in the first 125 ms after delivery of the tastant. The multiple pre-stimulus vertical gray lines in the bottom PSTH indicate the timing of cue presentation. Dashed horizontal lines: baseline firing frequency. The histograms to the right detail the response profile in the first bin. **G.** Trial-by-trial population activity in the first 125 ms bin. Color plots display representative dissimilarity matrices for trials in response to UT (left) and ExpT (right). Color coded squares represent the Euclidean distance between population vectors for different trials in the same session (color bar on the right of each plot). The plots to the right of each dissimilarity matrix represent population activity for 10 neurons in 8 trials. The diameter of the circles is proportional to the normalized activity of each neuron in first bin (white circles: UT; gray circles: ExpT).

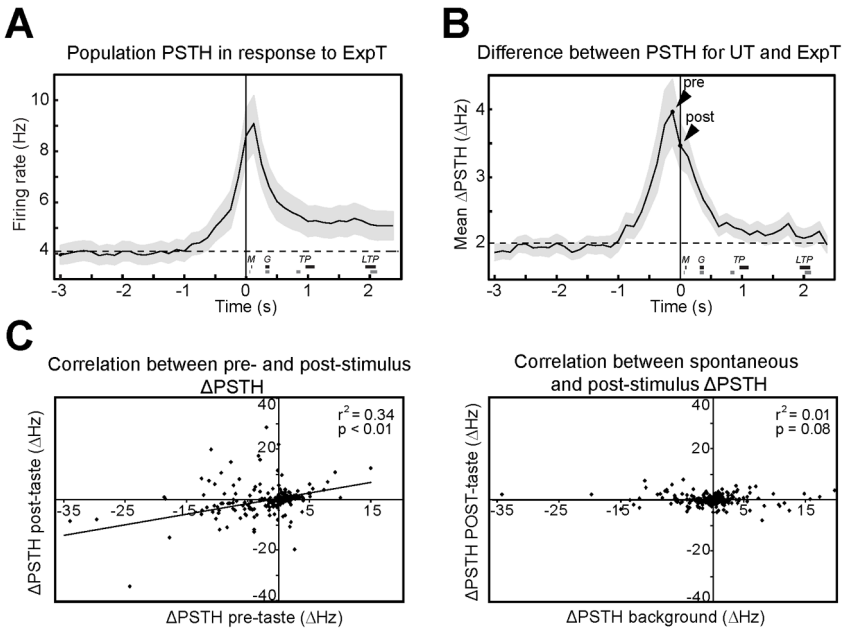

Figure 2.

Changes in taste-evoked activity correlate with anticipatory activity. **A.** Population PSTH in response to ExpT (bin width: 125 ms; n = 298 neurons). Shaded area around the trace represents SEM. Firing rates gradually elevate above baseline (the dashed line) before self-administration (t = 0). The thick horizontal bars labeled as M (minimal mouth movements), G (gapes), TP (small tongue protrusions) and LTP (lateral tongue protrusions) denote the average onset time (± SEM) for each oro-facial reaction in response to UT (black lines) and ExpT (gray lines). **B.** The average ΔPSTH (125 ms bin width, n = 298) in response to ExpT and UT shows a large pre-tastant increase (arrowhead "*pre*") relative to baseline (dashed line). Baseline difference was computed as the average ΔPSTH between 5 and 3 s prior to tastant delivery. Time 0 is when gustatory stimulation occurs; "*pre*" arrowhead indicates the last 125 ms bin before gustatory stimulation; "*post*" arrowhead indicates the first 125 ms bin after stimulation. Shading around the trace represents the SEM. Thick horizontal bars labeled as M, G, TP and LTP indicate the average onset time (± SEM) for oro-facial reaction in response to UT (black lines) and ExpT (gray lines). **C.** Left panel: linear regression analysis correlating the ΔPSTH in the last pre-stimulus bin with the ΔPSTH in the first post-stimulus bin. Each point represents a neuron from a sample of 298 cells recorded. Right panel: linear regression analysis between ΔPSTH in the first post-stimulus bin and ΔPSTH of a bin from background activity (i.e. randomly chosen in the interval between 5 and 3 s before tastant delivery). As expected, there is no correlation in this control condition.

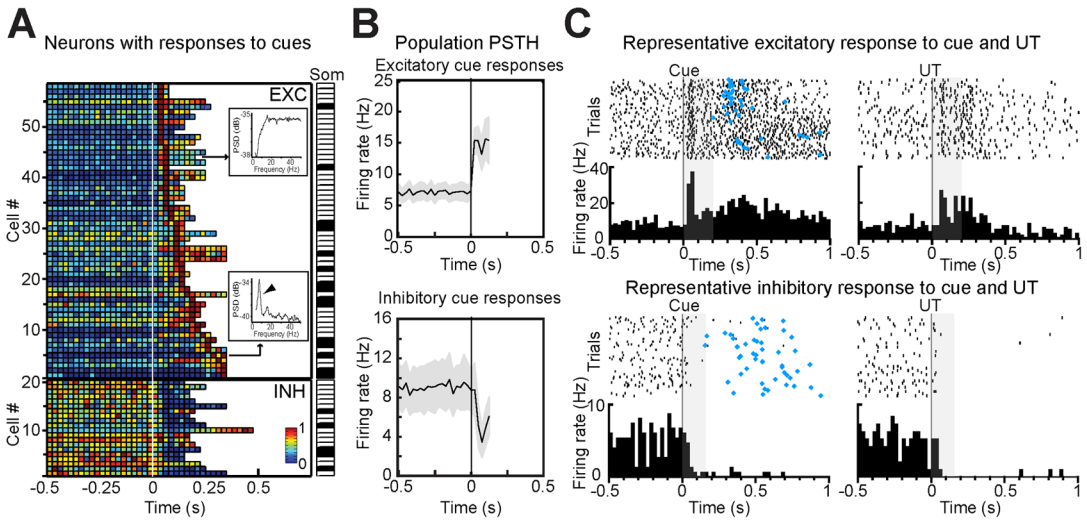

Figure 3.

Cue-evoked anticipatory responses in GC. **A.** Population plot of all the neurons producing significant responses to tones. Each row on the y-axis represents a neuron, the x-axis is time around cue onset (white line, t = 0), the color of each square describes the normalized firing rate within a 25 ms bin (see color bar). Top: neurons with excitatory responses (n = 58), bottom: inhibitory responses (n = 20). The insets show the power spectra for representative non-somatosensory (top) and somatosensory (bottom) neurons. The arrowhead in the power spectrum plot points to the peak in the licking frequency. The strip plot to the right ("Som") indicates the cells with (black) and without (white) a somatosensory peak. **B.** Population PSTH in response to anticipatory cues (0.5 s before to 125 ms after the cue; bin width = 25 ms). Top: average of neurons with no somatosensory peak showing excitatory responses (n = 43); bottom: average of inhibitory responses (n = 15). Gray shading around each trace: SEM; t = 0 is the onset of the cue. **C.** Raster plots and PSTH (25 ms bin width) for two representative neurons responding to the tone cue (left) and UT (right). Top: excitatory response; bottom: inhibitory response. The gray box marks the interval between the onset of the cue and the first lever press. Blue diamonds: time of lever press.

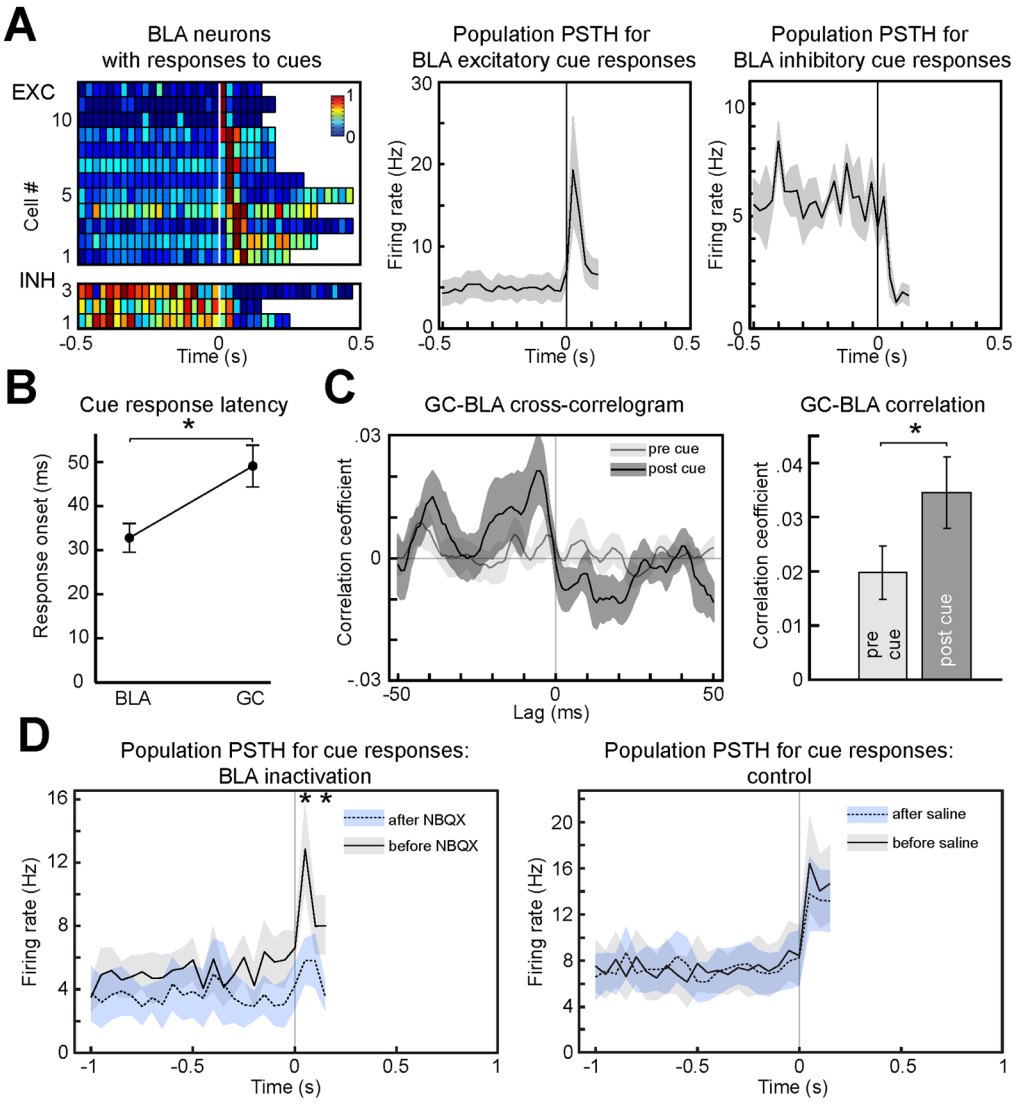

Figure 4.

Cue responses depend on top-down inputs from BLA. **A.** Population plot of cue responses for neurons in BLA (left panel top: excitatory responses; bottom: inhibitory responses). Details of the plot are as in Figure 3A. Right panel: average PSTH for all the excitatory (middle, n = 12) and inhibitory (right, n = 3) responses (bin width = 25 ms). **B.** Latency of cue response in BLA and GC (n = 15 and n = 56 respectively). **C.** Spike-field correlation between cue-responsive excitatory BLA neurons and GC LFP. Dark gray: first 125 ms following the presentation of the cue (post-cue); light gray: 125 ms before cue (pre-cue). Left panel: a representative cross-correlogram before and after the presentation of the cue. Note the higher peak after cue presentation. Right: histograms of the average peak correlation within ± 50 ms lag for activity before and after cue. The asterisk in **B** and **C** indicates significant differences. **D.** Effects of BLA pharmacological inactivation on cue responses in GC. The left panel shows population PSTH (bin width = 25 ms) for cue-evoked activity before (solid line and gray shading) and after (dotted line and blue shading) BLA infusion of NBQX (n = 5). The asterisk above traces indicates the bins at which responses before and after NBQX are significantly different. The right panel shows how saline

infusion has no effect on cue responses in GC (n = 12). The shading around each trace represents the SEM.

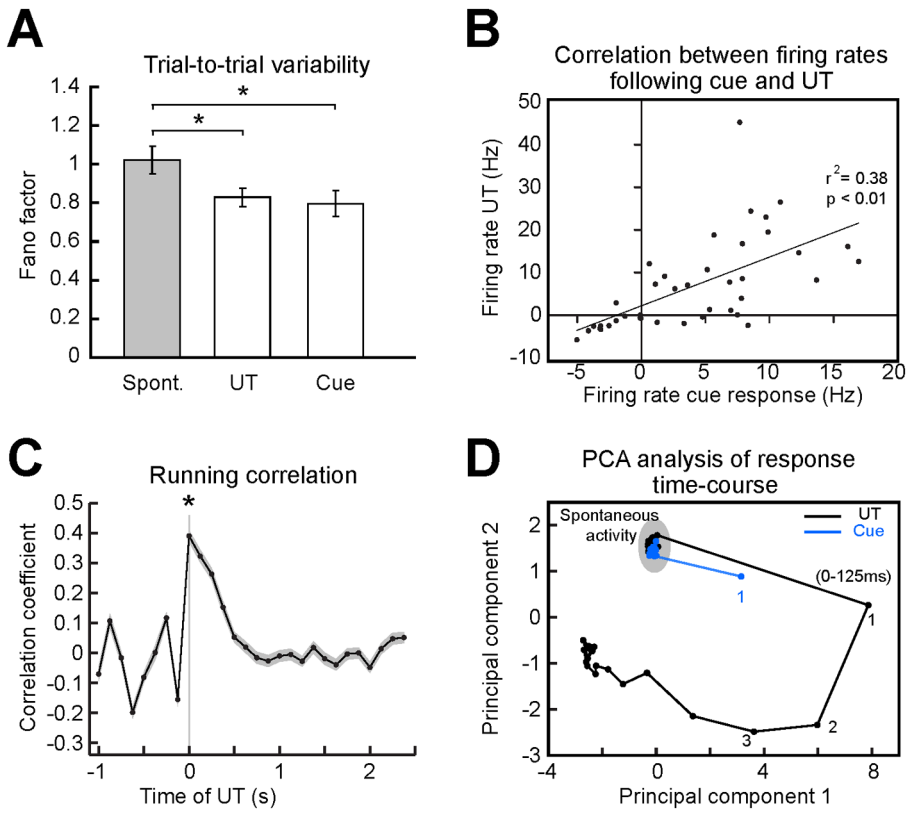

Figure 5.

Cue responses anticipate activity evoked by UT. **A.** Fano factor analysis for all the non-somatosensory neurons that showed excitatory cue responses (n = 43) computed in three conditions: spontaneous activity, first 125 ms following the cue and for first 125 ms after UT. The reduction in variability evoked by tastants and cues was not significantly different. **B.** Correlation between firing rates in the first 125 ms following the cue and firing rates in the first 125 ms following UT. **C.** Trial-averaged running correlation between the population firing patterns evoked by the cue in the first 125 ms and the time course of the population response to UT. Shaded area: SEM. **D.** PCA based visualization of the population activity in response to cues (blue line and dots) and UT (black line and dots); numbers indicate the order of 125 ms wide bins following stimulation. The asterisks in **A** and **C** indicate significant differences. Analyses in **B**, **C** and **D** are limited to putative pyramidal neurons (n = 40).

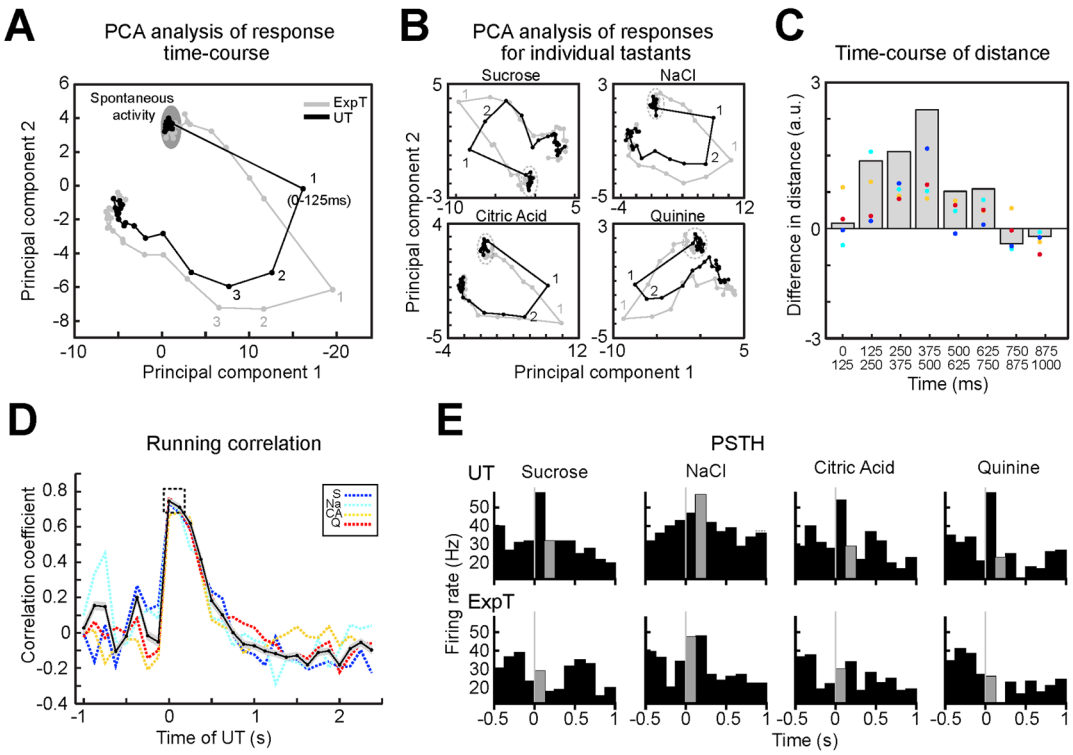

Figure 6.

Expectation changes the time-course of sensory responses in the subpopulation of pyramidal neurons. **A.** PCA based visualization of population activity evoked by ExpT (gray) and UT (black). Note that the first bin of the response to ExpT (1st gray) gets closer to the second bin evoked by UT (2nd black). **B.** PCA analysis for individual tastants confirms the same patterns as in panel **A. C.** Difference between the distance in a PCA space of homologous bins (i.e. 1st–1st) and successive bins (i.e. 1st–2nd) in the two conditions. Gray histogram: difference for trajectories averaged across tastants; color coded dots: difference for each tastant (same colors as in panel D). **D.** Trial averaged running correlation between population activity evoked by ExpT in the first 125 ms and the time course of the average response to UT. Black solid line: average across tastants; the shading around the black solid line represents the SEM of the difference; color coded dashed lines: data for each tastant (S = Sucrose - blue; Na = NaCl - cyan; CA = Citric Acid - yellow; Q = Quinine - red). The dashed box highlights the wide correlation with the first and second bin after UT. **E.** Example of a single neuron whose initial response to the ExpT (gray portion of the PSTH below) is similar to the response produced in the second 125 ms by UT (gray portion in the PSTH above); taste stimulation is at t = 0. The population used for this figure is the same as for Figure 5B, C and D (i.e. putative pyramidal neurons, n = 40).